Environ Monit Assess (2011) 180:409–426
DOI 10.1007/s10661-010-1796-6

Ion chemistry and individual particle analysis of atmospheric aerosols over Mt. Bogda of eastern Tianshan Mountains, Central Asia

Shuhui Zhao · Zhongqin Li · Ping Zhou

Received: 27 March 2010 / Accepted: 9 November 2010 / Published online: 25 November 2010

Abstract Aerosol samples were collected during the scientific expedition to Mt. Bogda in July–August, 2009. The major inorganic ions (Na^+, NH_4^+, K^+, Mg^{2+}, Ca^{2+}, Cl^-, SO_4^{2-}, and NO_3^-) of the aerosols were determined by ion chromatography. SO_4^{2-}, NO_3^-, and Ca^{2+} were the dominate ions, with the mean concentrations of 0.86, 0.56, and 0.28 μg m^{-3}, respectively. These mean ion concentrations were generally comparable with the background conditions in remote site of Xinjiang, while much lower than those in Ürümqi. Morphology and elemental compositions of 1,500 particles were determined by field emission scanning electron microscopy equipped with an energy dispersive X-ray spectrometer. Based on the morphology and elemental compositions, particles were classed into four major groups: soot (15.1%), fly ash (4.7%), mineral particles (78.9%), and little other matters (0.8% Fe-rich particles and 0.5% unrecognized particles). Presence of soot and fly ash particles indicated the influence of anthropogenic pollutions, while abundance mineral particles suggested that natural processes were the primary source of aerosols over this region, coinciding with the ionic analysis. Backward air mass trajectory analysis suggested that Ürümqi may contribute some anthropogenic pollution to this region, while the arid and semi-arid regions of Central Asia were the primary source.

Keywords Aerosols · Ion chemistry · Individual particle analysis · FESEM-EDX · Mt. Bogda

S. Zhao (✉) · Z. Li · P. Zhou
State Key Laboratory of Cryospheric Sciences/Tianshan Glaciological Station, Cold and Arid Regions Environmental and Engineering Research Institute, Chinese Academy of Sciences, Lanzhou 730000, China
e-mail: shuhui.zhao@163.com

Z. Li
Northwest Normal University, Lanzhou 730030, China

Introduction

Aerosol particles are ubiquitous in the atmosphere and exert an important influence on global climate and the environment. They affect the Earth's radiation budget, and hence climate, directly through the scattering, and absorption of light and indirectly by acting as cloud condensation nuclei (Buseck and Pósfai 1999). Increasing attention has been devoted to the study of aerosols; however, they still represent a major uncertainty in the knowledge of climate change due to high spatial and temporal variability in their atmospheric loading and properties. Thus, detailed information on chemical and physical properties is

important for the aerosol studies. Water-soluble ions comprise a large part of aerosol particles and play an important role in the atmosphere. Knowledge of the water-soluble ions of aerosols can provide information on the effect of regional and local pollution on the ecosystem health (Wang et al. 2005). Meanwhile, individual-particle analysis through scanning electron microscopy equipped with energy dispersive X-ray instrument (SEM/EDX), can provide a great amount of information that cannot be obtained though bulk ionic analysis (e.g., Shi et al. 2003; Reid et al. 2003; Gao et al. 2007; Srivastava et al. 2009). It can provide specific information on particle size, morphology, elemental composition, as well as surface coatings and agglomeration (Paoletti et al. 2002). Such analysis approaches can complement each other, giving a more clear view of aerosol properties. While combined analysis has been widely used to study aerosols in urban areas and some other area (e.g., Yue et al. 2006; Sharma and Srinivas 2009; Cong et al. 2010), little is conducted over Central Asian alpine site, especially in the Tianshan Mountains.

The Tianshan Mountains (Tianshan), located at the center of the arid and semi-arid regions of Central Asia, contains the most inland glaciers in the world. Dust storms (Asian dust) originating from the region are transported eastward, on a hemispheric scale, impacting eastern China, North and South Korea, Japan, and the USA as well. Transport and deposition of the dust plays a significant role in the biogeochemical cycles and atmospheric chemistry of the northern hemisphere (Arimoto et al. 2006). Mt. Bogda with the highest elevation of 5,445 m above sea level (a.s.l.) over the eastern Tianshan provides a unique opportunity to improve our understanding of the long-distance transport aerosols in the free troposphere, which have potentially significant impacts on regional and global climate. In addition, Mt. Bogda lies approximately 60 km east and commonly downwind from Ürümqi, the provincial capital of Xinjiang Uygur Autonomous Region with more than two million inhabitants, which has been heavily air-polluted and evaluated as one of the 10 heaviest air polluted cities over World for the past two decades (Mamtimin and Meixner 2007). Aerosols collected from this area can also give the opportunity to study the influence of anthropogenic pollution on the remote area of eastern Tianshan, which has been debated over the past several years (e.g., Wake et al. 1992; Williams et al. 1992; Sun et al. 1998; Hou et al. 1999; Lee et al. 2003; Zhao et al. 2008).

Due to the atrocious transport condition and working environment near Mt. Bogda on the eastern Tianshan, studies on atmospheric chemistry have been very limited to date on both temporal and spatial scales. Two 0.5 m snowpits were drilled in 1989 near Bogda Peak. Ion chemistry studies of the snowpits suggested that anthropogenic pollutions from Ürümqi had affected the higher concentration of sulfate on the glacier (Wake et al. 1992). However, there is no data reported to reflect the air conditions directly, and only using sulfate concentrations in snow to deduce the anthropogenic pollution is insufficient (Cong et al. 2010).

In order to obtain an updated knowledge of the air conditions, an intensive sampling experiment for aerosol was conducted during the scientific expedition to Mt. Bogda on the eastern Tianshan from July 26 to August 4 in 2009. The purposes of this study are to understand the inorganic ion chemistry properties of the aerosols, determine the elemental compositions and morphological properties of individual aerosol particles, identify their sources of origin, and evaluate the influence of the anthropogenic pollutions on the atmosphere over Mt. Bogda. The intensive sampling of 10 days will help to understand the characteristics of aerosols in summer time, which is included in the low dust periods (July to January). Although the field experiment covered only 10 days, inorganic ion chemistry and individual analysis of aerosols here was attempted to be investigated for the first time.

Sampling and analysis

Site description

Eastern Tianshan is one of the most arid and far inland glacierized regions in the world. Mt. Bogda with the highest elevation of 5,445 m a.s.l. over the eastern Tianshan, in particular, is just like

an island surrounded by a sea of desert (Fig. 1). In addition, Mt. Bogda lies approximately 60 km east from Ürümqi, the capital city of Xinjiang Uygur Autonomous Region. Both sides of Mt. Bogda were controlled by the cold Mongolia high pressure in winter and the westerly jet prevail high above the mountains during summer (Wu et al. 1983). Study of the aerosol characteristics under such geographic and climatic conditions will help us to understand the natural dust and anthropogenic influence, which might be partly responsible for the air quality of this glacierized region. In this work, aerosol samples were collected on the terminal moraine (43°48′ N, 88°16′ E, 3,546 m a.s.l.) of Bogda Fan-Shaped Diffluence Glacier, which distributed on the northern slope of Mt. Bogda. Because high altitude from 3,000 to 12,000 m a.s.l. is considered to be the mid- and top-troposphere over Tianshan Mountains (Hu 2004), the sampling site in our study is considered to be under the influence of the free troposphere, and sometimes receive the upper air mass transported in the free troposphere. Bogda Fan-Shaped Diffluence Glacier occupies a total area of about 10.94 km^2. The firn line has averaged around 3,800–3,900 m a.s.l. and the altitude of the end of the glacier was 3,620 m a.s.l. During the past decades, the glacier had shrunk and retreated greatly (Li et al. 2010).

Aerosol sampling

Daily aerosol samples of total suspended particles (TSP) were collected for a 10-days period from July to August in 2009. Aerosol samples were recovered on Zefluor™ Teflon filters (2.0-μm pore size, 47 mm diameter, Gelman Sciences) using a 12-V diaphragm pump powered by solar cells. Filters were loaded in the field and mounted face down about 1.5 m above the ground surface.

The air volume through the filter was measured by an in-line meter and then converted into standard conditions according to the local ambient pressure and temperature. The particle collection efficiency (for particles as small as 0.035 μm) was estimated to be >97% based on the mean flow rate of 1.27 m^3 h^{-1} over the filter (Liu et al. 1984). The sampling period for each aerosol sample was 3–12 h with sampling starting at 8:00 a.m. to 14:00 p.m. (Beijing Time) depending on weather conditions. No samples were collected

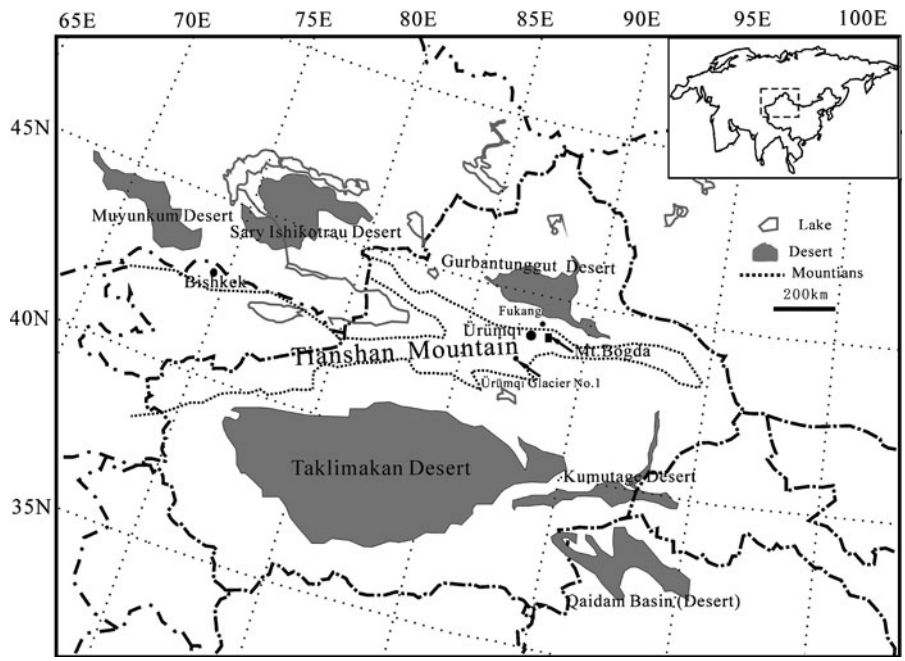

Fig. 1 Location map of Mt. Bogda with geographic environment around the eastern Tianshan

Table 1 Meteorological status during the sampling period

Parameters	Units	Mean	Range
Air pressure	hPa	661.4	657.6–663.6
Temperature	°C	4.7	1.4–7.7
R.H.	%	57	27–82
Wind speed	m/s	4.8	0.6–11.9

during rain/snow events. After sampling, filters were removed from the filter holder into cleaned airtight plastic containers and stored at 4°C before analysis. When loading or unloading the filters, the operator wore plastic gloves and faced upwind in order to minimize contamination.

An automatic weather station (AWS, Vantage Pro2 Plus, Davis Company, USA) was placed at the pass near the aerosol sampling site. Meteorological parameters, including air temperature, wind speed and direction, precipitation, air pressure, and relative humidity were measured simultaneously. The measurement resolution and uncertainties of these parameters are 0.1°C (±0.5°), 0.1 m/s (±5%), 22.5° (±4°), 0.2 mm (±4%), 0.1 hPa (±1 hPa), and 1% RH (±3%), respectively. The actually measured meteorological parameters were summarized in Table 1. The prevailing winds were from northwest (Fig. 2) during the sampling period.

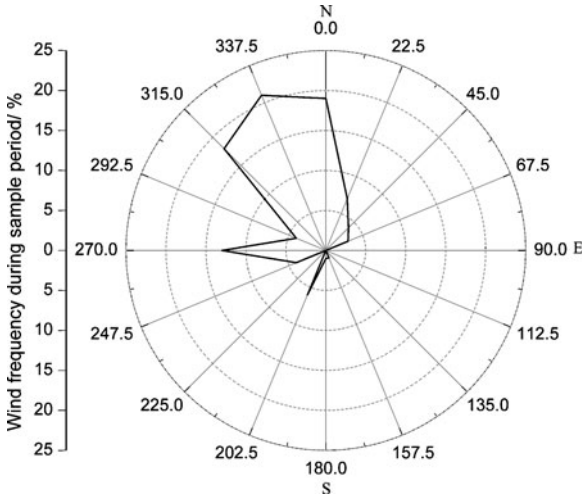

Fig. 2 Frequency of wind direction during the sampling period at Mt. Bogda

Sample analysis

All aerosol samples were analyzed in the clean room of 100 class, using a Dionex Ion Chromatograph model DX-320. To sufficiently extract the water soluble ions from the Teflon aerosol filters, each filter was wetted by 200 μl ultrapure methanol firstly, and then extracted with 25 ml aliquots of ultra-deionized water for about 1 h using an ultrasonic water bath device (e.g., Sun et al. 1998; Zhao and Li 2004; Zhang et al. 2008). After that, eight major inorganic ions (Cl^-, NO_3^-, SO_4^{2-}, Na^+, NH_4^+, K^+, Mg^{2+}, and Ca^{2+}) of the aerosols were analyzed. The chromatography conditions were as follows: for cations, CS12A analytical column, 15 mmol/L methane sulfonic acid eluent, cation self-regenerating suppressor, and 200 μl sample injected; for anions, AS11-HC analytical column, 12 mmol/L NaOH eluent, anion self-regenerating suppressor, and 200 μl sample injected. Average concentrations of 10 laboratory blanks were (in ng/g): Cl^- (3.66), NO_3^- (17.3), SO_4^{2-} (2.60), Na^+ (2.61), NH_4^+ (3.25), K^+ (0.04), Mg^{2+} (2.44), and Ca^{2+} (6.41), which were obviously lower than the concentrations detected in aerosol samples. Mean blank values were subtracted from sample concentrations. Then the sample concentrations were divided by the sample volumes (at standard conditions) of each sample and converted into micrograms per cubic meters, which were listed in Table 2. The precision, estimated from the standard deviation of repeat measurements of standards, was less than 6% for the measured ionic species; and the recovery of each ion was in the range of 90–106%. Detailed sampling methods and analytical techniques of aerosols are described by Zhao and Li (2004).

Because the Teflon filters are not very convenient for individual particle analysis, Nuclepore membrane filters with pore size of 0.4 μm (47 mm diameter, Whatman, UK) were used to study the individual particles. After 400 μl sample solution injected into the ion chromatography, 15 ml of each remainder solution of aerosol samples was filtered with a Nuclepore membrane under laminar flow immediately, and then air-dried in the 100-class ultra-clean chamber. We assume that, during the sample preparation, particles as the soluble part are completely removed

Table 2 Concentrations and ion balances of the water-soluble inorganic ions over Mt. Bogda

Date	Ion concentrations (μg m^{-3})								Σ^+ (μeq m^{-3})	Σ^- (μeq·m^{-3})	Σ^+/Σ^-
	Cl^-	NO_3^-	SO_4^{2-}	Na^+	NH_4^+	K^+	Mg^{2+}	Ca^{2+}			
7-26	0.029	0.283	0.346	0.051	0.032	0.053	0.008	0.181	0.015	0.013	1.15
7-27	–	0.171	0.960	0.141	0.034	0.193	–	0.262	0.026	0.023	1.13
7-28	0.008	0.114	0.252	0.040	0.019	0.036	0.004	0.138	0.011	0.007	1.57
7-29	0.112	1.315	1.820	0.165	0.264	0.267	0.008	0.541	0.056	0.062	0.90
7-30	0.063	1.114	0.504	0.119	0.023	0.194	0.005	0.129	0.018	0.030	0.60
7-31	0.001	–	0.180	0.015	0.014	0.020	–	0.043	0.004	0.004	1.00
8-1	0.044	0.248	0.751	0.104	0.066	0.121	–	0.217	0.022	0.021	1.05
8-2	0.035	0.322	0.983	0.100	0.135	0.060	0.020	0.376	0.034	0.027	1.26
8-3	0.035	0.745	1.234	0.045	0.232	0.074	0.018	0.362	0.036	0.039	0.92
8-4	0.149	1.318	1.543	0.290	0.065	0.321	–	0.539	0.051	0.058	0.88
Mean	0.048	0.563	0.857	0.107	0.088	0.134	0.006	0.279	0.027	0.028	1.05
SD	0.049	0.514	0.557	0.080	0.092	0.104	0.007	0.171	0.017	0.020	0.26
Min	0.001	0.114	0.180	0.015	0.014	0.020	0.004	0.043	0.004	0.004	0.60
Max	0.149	1.318	1.820	0.290	0.264	0.321	0.020	0.541	0.056	0.062	1.57
Max/min	149	12	10	19	19	16	5	13	14	16	3

from the insoluble part, which is also the basic principle to analyze the water soluble ions. This filtration method has already been widely used to study the individual aerosol particles recorded in snow and ice cores (e.g., Cong et al. 2009; Laluraj et al. 2009). For each Nuclepore membrane, section of the total filter was cut and mounted onto the electron microprobe stub, and coated with a thin gold film (16 nm) for better conductivity and a higher quality secondary electron image. The signal of Au in the EDX diagrams is appeared at the fixed opposition, and the gold film was too thin to prevent proper identification of the other elemental compositions. In our study, individual particles were analyzed using a Field Emission Scanning Electron Microscope JEOL JSM-6701F (FESEM) equipped with an energy-dispersive X-ray spectrometer (EDX/EDS). Operating conditions were: accelerating voltage = 5 ∼ 10 kV; spectral acquisition times = 60 s. X-ray analysis was carried out with a conventional Si (Li) detector with a Be window capable of detecting elements with atomic numbers ≥11. Noran System software for energy-dispersive microanalysis was used for the quantitative analysis of individual particles. The weight percent of elements was calculated based on characteristic X-rays. Approximately 1,500 individual aerosol particles from 10 samples were examined using the FESEM-EDX technique.

Results and discussion

Ion chemistry of aerosols over this region

Concentrations of water-soluble inorganic ions in total aerosols

A total of 10 aerosol samples were collected during the scientific expedition to Mt. Bogda. To provide a general indication of the chemical composition characteristics, daily variations of the concentrations for the major inorganic ions (Na^+, NH_4^+, K^+, Mg^{2+}, Ca^{2+}, Cl^-, SO_4^{2-}, and NO_3^-) are shown in Table 2. Of all anions, sulfate was the dominant component followed by nitrate, while concentration of chloride was much lower. The concentration of SO_4^{2-} varied from 0.18 to 1.82 μg m^{-3}, with the mean value of 0.86 ± 0.56 μg m^{-3}, while concentration of NO_3^- varied from 0.11 to 1.32 μg m^{-3}, with the mean value of 0.56 ± 0.51 μg m^{-3}. Mean concentration of Cl^- was about 0.05 ± 0.05 μg m^{-3}. With respect to cations it could be found that calcium was the most prominent component. The concentration of Ca^{2+} varied from 0.04 to 0.54 μg m^{-3}, with the average value of 0.28 ± 0.17 μg m^{-3}; while concentrations of the other analyzed cationic species (K^+, Na^+, NH_4^+, and Mg^{2+}) had the lower level of concentrations, which was about 0.006–0.13 μg m^{-3} on average.

To evaluate the acid-base balance of aerosol particles over this region, we converted the ions' mass concentrations into equivalent concentrations (μeq m^{-3}) as follows:

$$\sum{}^{+} = Na^{+}/23 + NH_4^{+}/18 + K^{+}/39 + Mg^{2+}/12 + Ca^{2+}/20 \quad (1)$$

$$\sum{}^{-} = Cl^{-}/35.5 + NO_3^{-}/62 + SO_4^{2-}/48 \quad (2)$$

And then the ratios of the sum of the equivalent concentrations of cations to anions (Σ^{+}/Σ^{-}) were calculated and presented in Table 2. The ion balance expressed by the sum of the concentrations of anion-to-cation is a good indicator to study the acidity of the environment (e.g., Wang et al. 2005; Wu et al. 2006; Khoder and Hassan 2008; Shen et al. 2009; Verma et al. 2010).

From Table 2, it was found that the ratio calculated for the entire aerosol samples ranged from 0.60 to 1.57. Such shifts in the ion balance are probably attributed to the different air masses that arrived at the sampling site, which resulted in the different air conditions (acidic or alkaline) by different origin (natural or anthropogenic sources). The Σ^{+}/Σ^{-} ratios for the aerosol samples on July 29–30 and August 3–4 were smaller than 1.0, which indicated that these samples were acidic. This is possible due to the much more increasing of NO_3^{-} and SO_4^{2-} than the cations. The Σ^{+}/Σ^{-} ratios for the aerosol collected on July 31 was 1.0, suggesting that aerosol particles in this day were almost neutral. The ratios of the other samples were more than 1.0, indicating that they were more alkaline. The mean ratio of 1.05 was close to 1, indicating that almost all of the ions had been quantified. When the total equivalents of anions were plotted against the total equivalents of cations, the slope of the regression line was slightly lower than unity (Fig. 3, slope = 0.83, R = 0.96), which implies cation deficiencies. It might be attributed to H^{+}, which was not counted in the calculation, or due to parts of NH_4^{+} that was probably vaporized into the gas phase (Wang et al. 2005, 2006; Shen et al. 2009). High temperature is probably the primary reason for the vaporization or volatilization of NH_4^{+} (Khoder and Hassan 2008). However, the lower temperature over this glacierized region (Table 1) may contribute little vaporization or volatilization of NH_4^{+} in our samples. Organic ions are another important constituent of the aerosol particles, the lack of the organic ions would cause some estimated errors of the ion balances. Due to the ions like formate, acetate, and other organic acid ions will contribute to the sum of the equivalent concentration of anions Σ^{-}, the real values of the Σ^{+}/Σ^{-} ratios will become smaller. Therefore, the larger values of the Σ^{+}/Σ^{-} ratios on several days are probably attributed to the organic ions (formate, acetate, etc.), carbonate, bicarbonate, F^{-}, NO_2^{-}, PO_4^{3-}, and Br^{-} were not determined in the present study (Wang et al. 2005; Khoder and Hassan 2008).

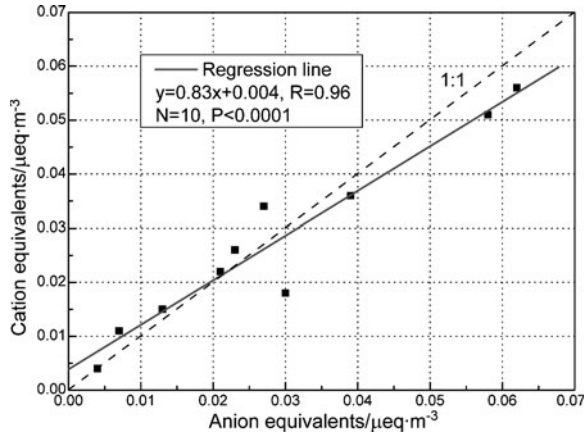

Fig. 3 Ion balance of the major water-soluble inorganic ions in the aerosols over Mt. Bogda

Correlation between ionic species in aerosols

To identify and separate the impact of various sources, correlation coefficients between the ionic species were calculated and shown in Table 3. Significant positive correlation coefficients were found between Ca^{2+} and SO_4^{2-} (r = 0.964 at p = 0.05), while Ca^{2+} also correlates well with Na^{+}, K^{+}, Cl^{-}, and NH_4^{+}. Due to calcium is usually rich in the desert and loess soils and even the atmospheric aerosol particles collected from the desert and loess areas, Ca^{2+} was always accepted as a proxy for dust in the studies of snow and ice chemistry (e.g., Mayewski et al. 1993; Wolff 1996). Previous studies over

Table 3 Inter-species correlation coefficients

	Cl^-	NO_3^-	SO_4^{2-}	Na^+	NH_4^+	K^+	Mg^{2+}	Ca^{2+}
Cl^-	1.000	0.902*	0.738**	0.843*	0.384	0.832*	−0.064	0.773*
NO_3^-		1.000	0.728**	0.709**	0.495	0.813*	0.082	0.697
SO_4^{2-}			1.000	0.714**	0.772*	0.742**	0.235	0.964*
Na^+				1.000	0.130	0.934*	−0.268	0.736**
NH_4^+					1.000	0.229	0.630	0.718**
K^+						1.000	−0.324	0.687**
Mg^{2+}							1.000	0.304
Ca^{2+}								1.000

*$p = 0.05$; **$p = 0.01$

Tianshan Mountains found that the surrounding desert and arid regions were usually considered to be the primary sources of Ca^{2+} (e.g., Williams et al. 1992; Sun et al. 1998; Aizen et al. 2004; Zhang et al. 2008). Okada and Kai (2004) also found that the calcium-rich mineral particles in the desert usually present as $CaCO_3$, $CaSO_4$, and internal mixture of $CaCO_3$ and $CaSO_4$ or silicates. Therefore, significant correlation with Ca^{2+} suggests that SO_4^{2-} may also originate from the desert dust and existed as $CaSO_4$. Besides, evaporite deposits abundant in sulfate salts (including gypsum) existed in the regions to the west of Tianshan in the Aral Sea/Kuzul Kum desert region are another important natural sources of SO_4^{2-} (Kreutz and Sholkovitz 2000). Of course, oxidation of the SO_2 emitted from coal burning for house heating domestically and industries is another possible source of SO_4^{2-}. Ürümqi, which lies approximately 60 km away in the west of Mt. Bogda, has been heavily air-polluted by the heating with coal combustion (Mamtimin and Meixner 2007; Li et al. 2008). Although there was little house heating domestically in summer, coal burning for industries and other fossil fuels burning were still the potential pollution sources of SO_4^{2-} to this region. To separate anthropogenic source from natural source of SO_4^{2-}, the value of the equivalent concentration ratio of SO_4^{2-}/Ca^{2+} was calculated as described by Ming et al. (2007). High values of SO_4^{2-}/Ca^{2+} (43.2 and 138.8) in Mt. Qomolangma suggested that SO_4^{2-} have the major anthropogenic sources, while lower values (3.8) suggested the major dust sources (Ming et al. 2007). The values of SO_4^{2-}/Ca^{2+} in our samples only ranged from 0.8 to 1.8. Thus, it indicated that SO_4^{2-} in our samples was mainly controlled by the natural processes.

Significant positive correlation coefficients were also found between SO_4^{2-} and NH_4^+ ($r = 0.772$ at $p = 0.05$), suggesting the neutralization by ammonia gas to the exceeded SO_4^{2-}. The high correlation coefficients between each other of SO_4^{2-}, Ca^{2+}, and NH_4^+ concentrations indicate that the forms of $(NH_4)_2SO_4 \cdot CaSO_4 \cdot 2H_2O$ likely existed in the aerosols (Khoder and Hassan 2008). The secondary aerosol $(NH_4)_2SO_4$ is usually formed by the oxidation of SO_2 to form the gas phase of H_2SO_4 and then reacted with NH_3. The formation was significant in summer due to the conversion of gaseous precursors (Wang et al. 2005). Ammonia (NH_3) was the most abundant gaseous alkaline component in the atmosphere. The potential sources for ammonia over this region are human and agriculture activities such as animal farming, fertilizers, and organic decomposition (Sun et al. 1998; Kreutz et al. 2001; Wu et al. 2006; Verma et al. 2010). Insignificant positive correlation coefficients were found between NH_4^+ and other ions, indicating that they were from different sources.

Na^+, K^+, and Cl^- show significant positive correlation coefficients with other ions except NH_4^+ and Mg^{2+}. High correlations with Ca^{2+} indicate that Na^+, K^+, and Cl^- may have the same desert sources. Halite (NaCl) particles were commonly detected in the aerosol particles collected over the Taklamakan Desert (Okada and Kai 2004). Wake et al. (1990) and Sun et al. (1998) have also pointed out Na^+ and Cl^- in the Tianshan represent an input of Na^+ and Cl^- rich dust originating from the extensive evaporate deposits in the arid regions surrounding these mountain ranges. Potassium is probably also derived from these evaporites, because it is higher correlations with sodium.

NO_3^- is almost the reaction product of NO_x emission, while the NO_x emission is mainly due to fossil fuel combustion and biomass burning (Wang et al. 2006; Wu et al. 2006). Under an alkaline atmospheric environment, gaseous HNO_3 formed by the oxidation of NO_x can be absorbed on the surface of mineral particles and reacted to form salts (Mamane and Gottlieb 1992). This may be the reason that NO_3^- has significant correlations with Na^+, K^+, and Cl^-. Previous studies found that automobile exhaust is a major contributor of NO_3^- (e.g., Arimoto et al. 1996; Wang et al. 2005, 2006; Khoder and Hassan 2008; Bhaskar et al. 2009). Glaciochemical investigation from Belukha glacier also pointed out that the increased nitrates resulted from the growth of traffic and the associated rise of the emission of precursor gases NO_x (Olivier et al. 2003). Therefore, the higher content of NO_3^- in our study is likely related to the anthropogenic pollutions, and traffic emissions from Ürümqi may be the potential source.

Comparison with data of the previous study and other areas

In our study, mean ion concentrations of aerosol samples were in the order of $SO_4^{2-} > NO_3^- > Ca^{2+} > K^+ > Na^+ > NH_4^+ > Cl^- > Mg^{2+}$, which was different from the chemical compositions of snowpits samples collected at this region in 1989 (Wake et al. 1992). For the snowpits samples, mean ion concentrations (in μg m^{-3}) followed the order SO_4^{2-} (3,355.2 μg m^{-3}) > Ca^{2+} (1,726 μg m^{-3}) > Na^+ (1,568.6 μg m^{-3}) > Cl^- (443.8 μg m^{-3}) > NO_3^- (328.6 μg m^{-3}) > Mg^{2+} (120 μg m^{-3}) > K^+ (113.1 μg m^{-3}). As the snowpacks in April 1989 represented approximately 6 months' accumulation including the winter of 1988 and spring of 1989, ion concentrations of the snowpits samples were much higher than that of our aerosol samples. Higher contributions of NO_3^- in aerosols than snowpits cannot be simply concluded as an increase in anthropogenic aerosol concentrations in this region between 1989 and 2009, due to the complicated air-to-snow-to-firn transfer processes. According to the study by Zhao et al. (2006), nitrate was found to be highly mobile in the snowpack, and appeared to be preferentially leached downward into the ice layer, thus, concentrations of NO_3^- seemed lower in snowpits. Due to the complicated transfer processes, only use the NO_3^- in snowpits cannot reflect whether there were anthropogenic pollutions affecting this region in 1989. Lower abundance of Ca^{2+} in aerosols is likely attributed to the low dust sampling period than spring. Due to the various sources (anthropogenic or crustal) of SO_4^{2-} in atmosphere (Ming et al. 2007), the similarity between the contributions of SO_4^{2-} in aerosols and snowpits samples cannot be just considered as a reliable proxy for anthropogenic emissions which was proposed by Wake et al. (1992).

We also compared the data with urban and background areas in Xinjiang to estimate the contributions of natural and anthropogenic sources. The comparison with the ion concentrations of TSP in Ürümqi (Li et al. 2008), the heavily air-polluted capital city of Xinjiang Uygur Autonomous Region, shows that the major ions (Na^+, NH_4^+, K^+, Mg^{2+}, Ca^{2+}, Cl^-, SO_4^{2-}, and NO_3^-) concentrations of aerosols over Mt. Bogda were 18 to 333 times lower than those in Ürümqi. Although the little higher concentrations of NO_3^- and NH_4^+ and exceed SO_4^{2-} over Mt. Bogda are likely attributed to the anthropogenic activates from Ürümqi, such low levels of ions concentrations than Ürümqi indicated that anthropogenic pollutions from Urumqi has not been a critical issue in the control of air quality of this region. Akdala (47°06′ N, 87°58′ E, 562 m a.s.l.), located at the northern Xinjiang, is a remote China Atmosphere Watch Network station, which has been shown to be minimally impacted by dust and local sources of pollution and is representative of "background" conditions in the mid-latitudes of northwestern China (Qu et al. 2009, 2010). If we accept an assumption that Akdala is representative of background conditions, we can compare samples from Mt. Bogda to the "background" condition, especially the ions might originated from anthropogenic activates. It can be found that except the higher concentrations of NO_3^- on July 29–30 and August 3–4, concentrations of SO_4^{2-}, NO_3^-, and NH_4^+ in our samples are lower than the mean concentrations of Akdala, which were 3.3, 0.58, and 0.60 μg m^{-3}, respectively. This comparison suggests that although anthropogenic

pollutions have some impact, ion concentrations of Mt. Bogda were comparable with the background conditions and natural processes were still the primary source of the aerosols.

Individual particles analysis

The final dataset included 1,500 particles analyzed on 10 filters. The particles were grouped into four

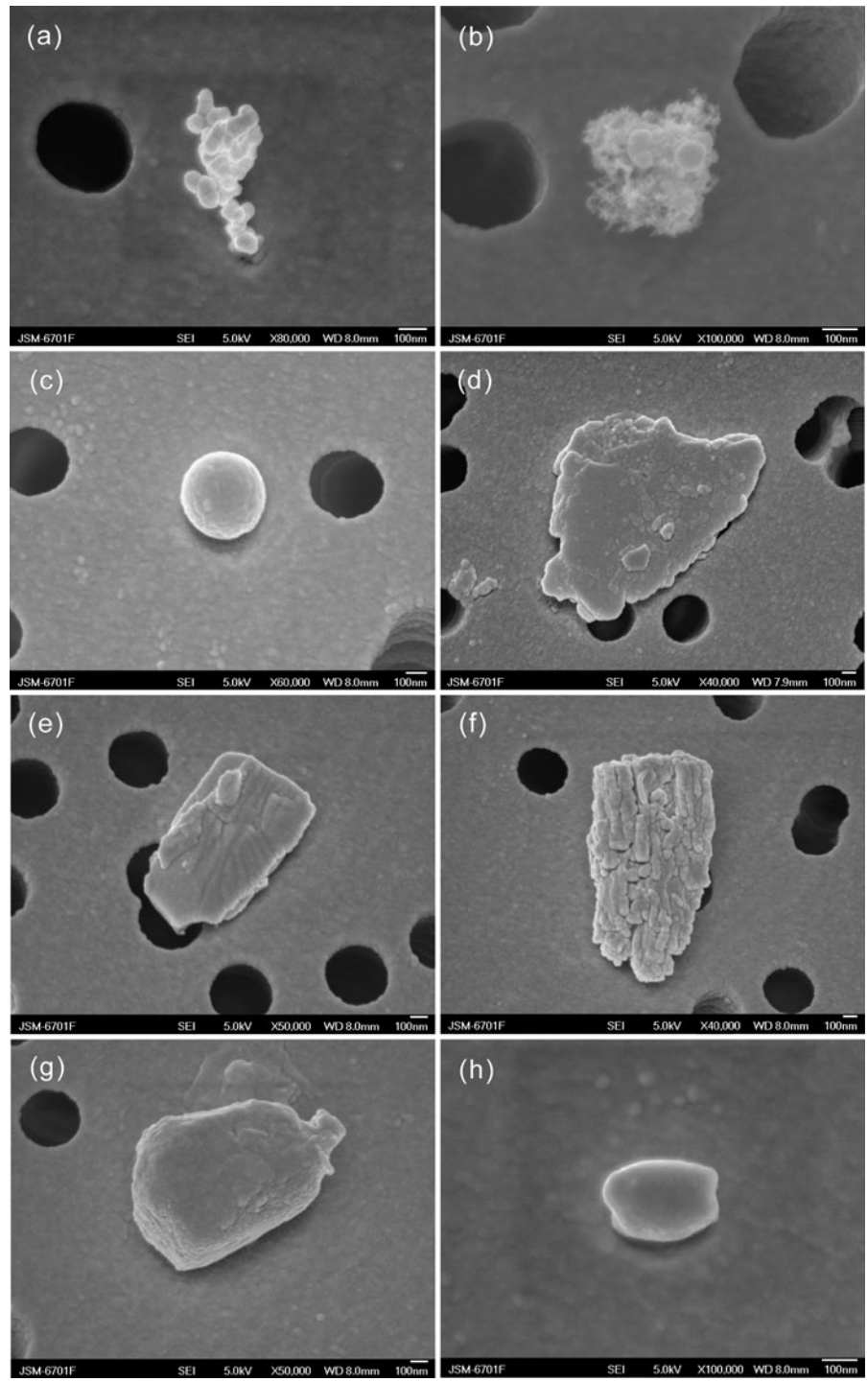

Fig. 4 FESEM images of typical aerosol particles: **a** chain-like soot aggregates; **b** soot aggregates (cluster); **c** spherical fly ash; **d** alumosilicate; **e** SiO_2; **f** calcium sulfate; **g** $CaCO_3$; **h** Fe-rich particles

dominant types according to their morphology and EDX signal. Figure 4 shows the typical individual particles loaded on the filters at different magnifications. The distinct characteristics and possible origins of each group are described in detail as follows.

Soot

Soot aggregates which account for about 15.1% were common in the samples. It could be easily recognized by its unique morphology as an agglomeration of spherical particles with diameters between 20 and 50 nm. In our study, soot particles consisted of two dominant morphological types: small chain of spherulites (Fig. 4a) and large aggregated clusters (Fig. 4b). The small chain may be recognized as the aged soot according the study by Hu et al. (2009). However, other studies also found that the morphology varies from short chains to complex clusters, which depend on different types of fuels, burning conditions, and atmospheric processing (Chakrabarty et al. 2006; Yue et al. 2006; Cong et al. 2010).

Soot particle (black carbon) is an incomplete-combustion product of biofuel, fossil fuel (e.g. petroleum, diesel, and etc.), and biomass burning (Ming et al. 2009). It is usually considered as the product of vehicle exhausts (gasoline or diesel) (Shi et al. 2003; Yue et al. 2006). Aerosol studies of Ürümqi found that soot, originated form the vehicle exhausts, was one of the abundant particles in the air (Li et al. 2005). Thus, the soot particles over Mt. Bogda may be transported from Ürümqi, which coincide with the ionic analysis and indicate the anthropogenic pollution during this period.

Due to the contribution to climatic change (global warming), reduced visibility, and adverse health effects, soot aerosol is drawing more and more attention from scientists. Studies found that soot aerosols deposited on glaciers have been a significant contributing factor to observed rapid glacier retreat (Ming et al. 2009; Xu et al. 2009). As relatively large amounts of soot particles were observed over Mt. Bogda, we hypothesize that it could be a potential contributor to the glacier recession in this region. However, further investigation is required to give a quantitative assessment of such influence.

Fly ash

Fly ash is characterized by a smooth spherical shape with the size larger than 100 nm (Fig. 4c). Chemical compositions of these particles were predominately aluminosilicates, which is similar to the soil particles (Xie et al. 2005, 2009). However, the soil particles usually have pronounced irregular shapes; the fly ash particles are, in most cases, nearly spherical. Generally, spherical particles are derived from fluid melts due to high-temperature combustion (Xie et al. 2005). Therefore, coal combustion and metallurgical plants are the main source of this type of particles. Aerosol studies of Ürümqi found that fly ash particles were abundant in winter, due to the coal combustion for house heating domestically (Li et al. 2005). In summer, metallurgical plants over Ürümqi still emit these particles, although the coal combustion for house heating has been terminated since April 16. That may be the illustration of the less percent (4.7%) of fly ash particles collected in our study.

Mineral particles

Mineral particles, comprising aluminosilicates, quartz, feldspars, gypsum, calcite, and etc., were the richest particles over this region. The sizes of mineral particles generally ranged from 0.5 to 11 μm. Although the sizes varied greatly, most of the particles fall in the range of 0.5–2.5 μm. The EDX spectra of aluminosilicates showed that they contain significant amounts of Si and Al, in addition to some other elements like Na, Mg, K, Ca, Ti, and Fe. In this study, particles contained mainly of Si–Al–Ca, Si–Al–K, Si–Al–Fe, and Si–Ca were also classified as aluminosilicates. Most of these particles were irregular shapes (Fig. 4d), suggested that they were from natural sources. Particles containing predominantly silicon were classified as quartz (SiO_2), with the irregular shape shown in Fig. 4e. As an important constituent of many rock types and dust, quartz is almost ubiquitous on land areas. In our study, alumosilicates and quartz were the major particles with average abundance of 59.6%. This is similar to the results of aerosols collected from high Himalayas (Cong et al. 2010) and a remote station in Kazakhstan over Tianshan (Hoornaert et al. 2004). These par-

ticles can mainly be attributed to the surrounded dust sources or Eolian dispersion of soil particles.

About 19.3% particles were identified with high abundances of Ca. Based on the EDX diagrams, these particles were then classified into two types: calcium sulfates characterized by high and approximately equal abundances of Ca and S, while calcium carbonates characterized by the only high relative X-ray intensities for Ca. Calcium sulfates originates usually from two sources: the primary natural source is gypsum, a typical mineral in the earth crust; another possible origin is through reactions of carbonates with sulfuric acid during transport (Gao et al. 2007; Cong et al. 2010). According to the irregular morphologies (Fig. 4f), calcium sulfates in our study were likely attributed to terrestrial sources, which existed as gypsum. These particles accounts for about 11.4%, which suggest that sulfate concentrations in snow from this area, cannot be just considered as a reliable proxy for anthropogenic pollution, special care should be taken to avoid misinterpretation. From the point of view of mineralogy, calcium carbonates (Fig. 4g) were probably in the form of limestone or calcite. Previous studies found that the region to the west of the Tianshan, between the Caspian and Aral Seas has the highest estimated amount of calcite on both a regional and global scale (Claquin et al. 1999). Aerosol particles collected from the desert and loess areas surrounding the Tianshan also contain a high mass proportion of Ca (Okada and Kai 2004). Therefore, these particles likely originated from local desert soils or through long-range transport from the west. However, an account of only 7.9% suggests the lower input of these particles during the low dust period.

Other particles

Other particles including Fe-rich particles and little unrecognized particles account for only 1.3%. Iron can originate from both natural and anthropogenic sources, e.g., from soil, mining, and ferrous metallurgic industry. Besides, contribution from coal combustion is also possible, and particles can be formed by oxidation of pyrite (FeS_2) in coal (Xie et al. 2009). Emitted by high-temperature furnaces, these particles are usually spherical (Cong et al. 2010). The almost spherical shaped particle with smooth edges and surface, shown in Fig. 4h, is therefore likely to have been emitted by a high temperature process. However, it may originate from the steel industry or from coal combustion. The unrecognized particles contained mainly organic particles with light elements (such as C, N, and O) or biological particles. As these particles account for only 0.5%, which is almost inexistent, they were remained unclassified.

In summary, ~78.9% of the detected particles over this region are probably from natural mineral dust, while ~21.1% of the particles may be emitted by anthropogenic activities. It suggests that natural processes were the primary sources, while some anthropogenic pollution also contributed to the aerosols over this glacierized site during the sampling period. Albedo of glacier is a very important factor to impact its mass balance besides net accumulation, air temperature, and flow dynamics. It was found that soot (black carbon) particles deposited on the surface of snow or ice could enhance solar radiation absorption, reduce the albedos intensively, and thus accelerate the melting of ice (e.g., Ming et al. 2009; Xu et al. 2009). However, Takeuchi and Li (2008) suggested that the albedo was also significantly reduced by the surface dust on the glacier and mineral dusts on the glacial surface substantially accounts for the shrinkage of the glacier. Consequently, further study is necessary to improve our understanding of which is sufficient to the enhanced melting and retreating of this glacier.

Relationships with air mass transport

To identify potential transport pathways and possible source regions of aerosols over Mt. Bogda, air mass back-trajectories were calculated by the Hybrid Single-Particle Lagrangian Integrated Trajectory (HYSPLIT) model of the Air Resources Laboratory of NOAA (Draxler and Rolph 2003). HYSPLIT back-trajectories have been widely used in previous studies (e.g., Marenco et al. 2006; Ming et al. 2007; Cong et al. 2010). In this paper, 5-day backward air trajectories were simulated with a daily resolution. Trajectories terminated at the sampling site (43°48′ N, 88°16′ E, 3,546 m a.s.l.) at the beginning time

(0:00 to 6:00 h UTC) of sampling were calculated every day. Meteorological data fields to run the model are available from the US National Centers for Environmental Prediction global data assimilation system. The vertical motion was calculated by the meteorological model's vertical velocity. The model output is a set of latitude–longitude coordinates of the air parcel estimated position with the 12-h time interval and pressure vertical coordinate.

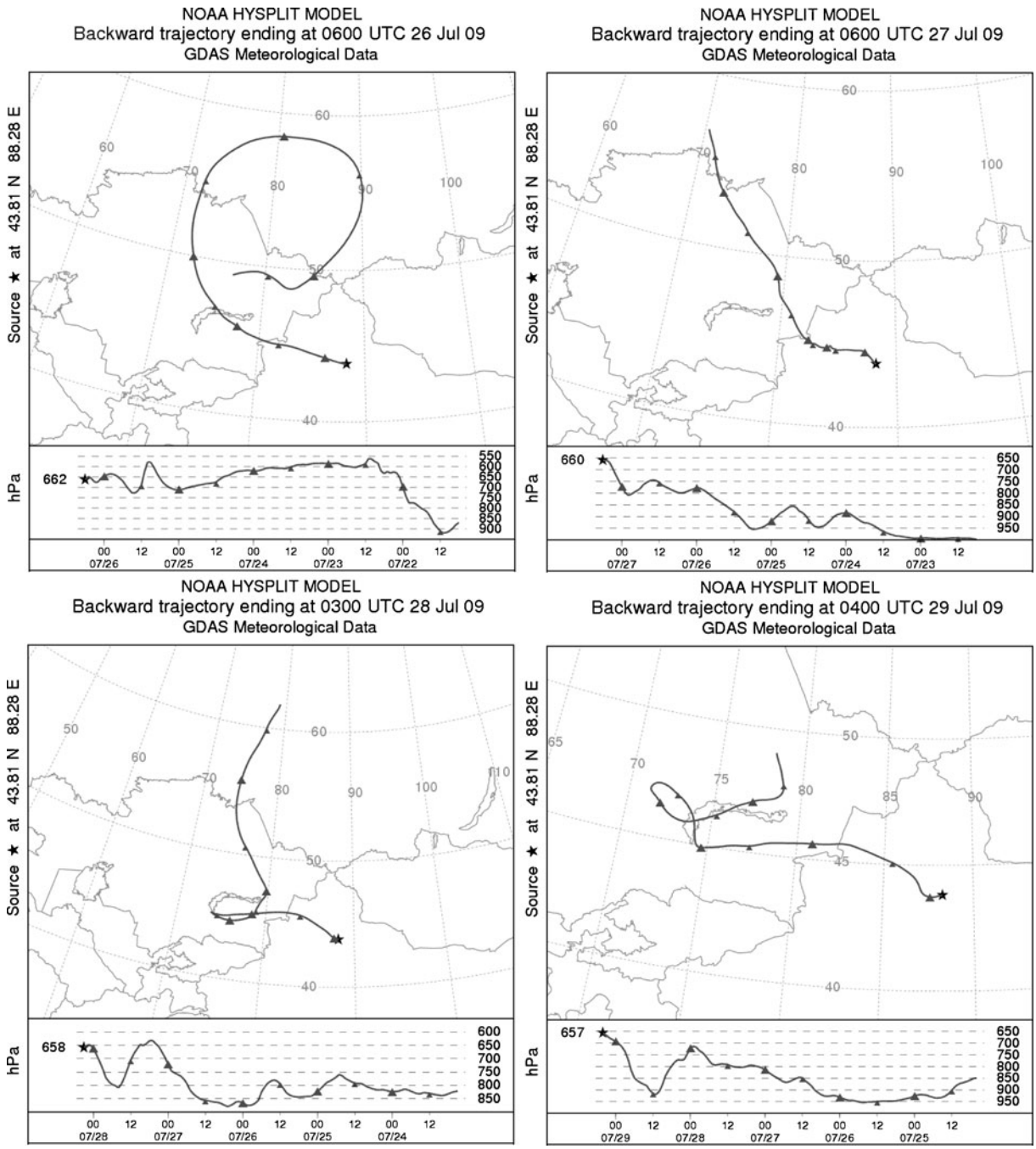

Fig. 5 Daily backward trajectories arriving at the sampling site

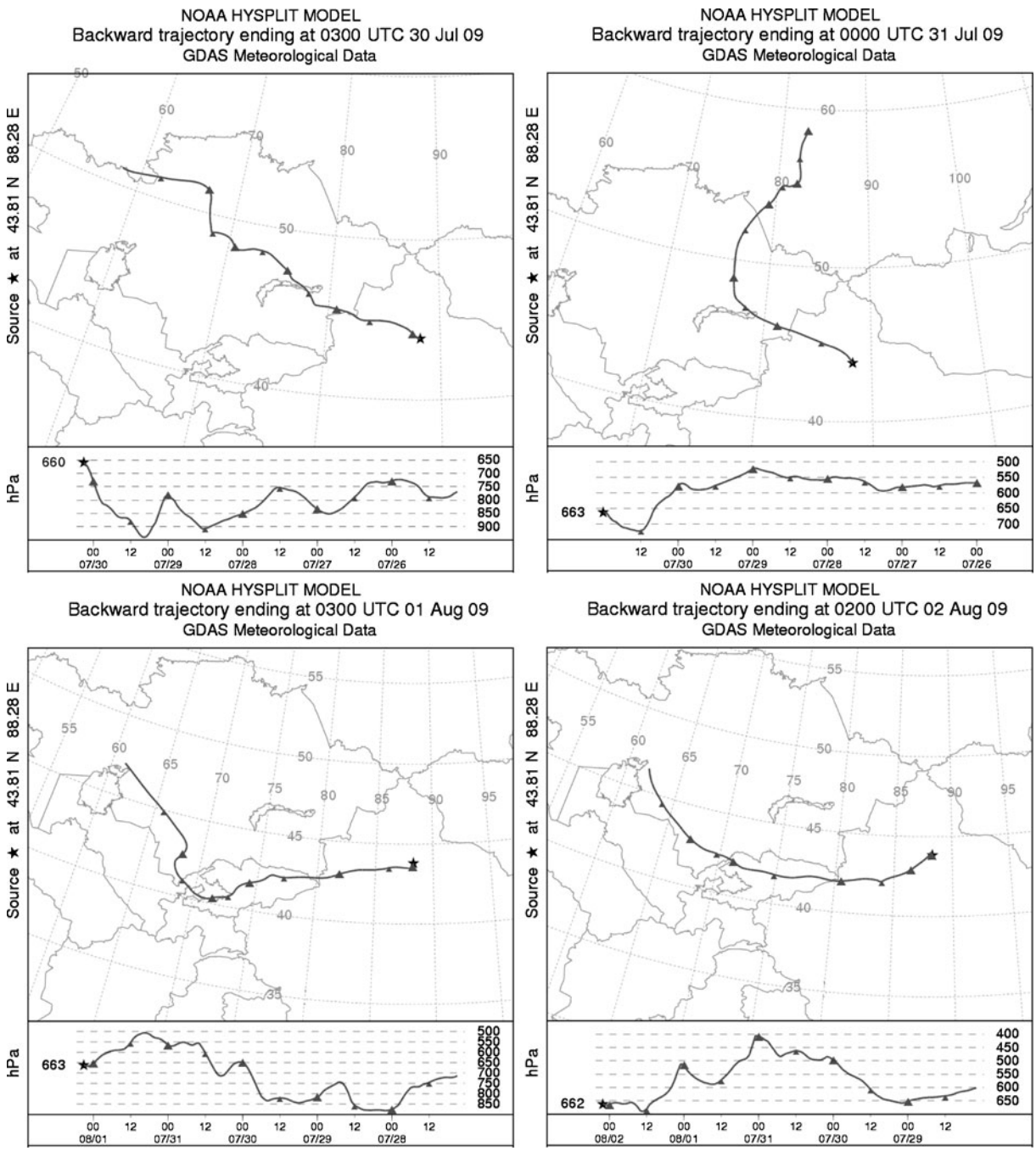

Fig. 5 (continued)

Figure 5 presents the daily backward trajectories during the sampling periods. Most of the air masses transported from west and northwest, agreeing well with the meteorological data. Combined with the ion concentrations listed in Table 2, air masses arriving at the sampling site can be classified into three types: (1) Air masses arrived at July 29–30 and August 3–4, originated from or transported through the arid regions of Kazakhstan, Kyrgyzstan, and Uzbekistan, and then

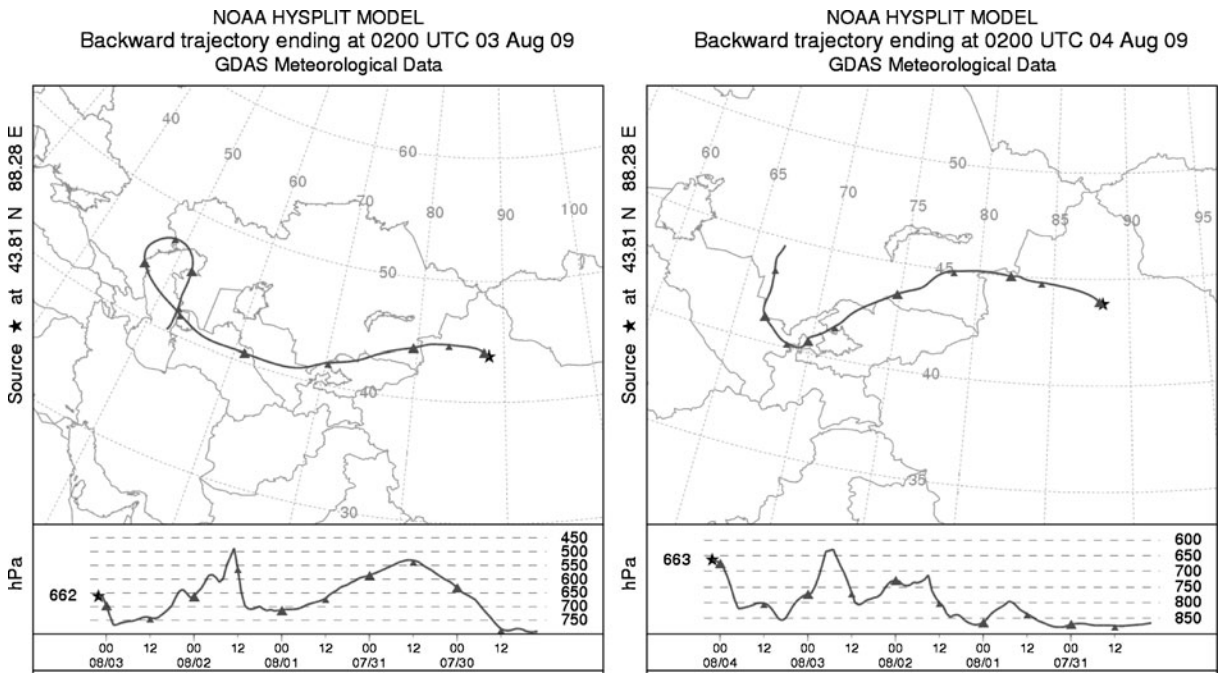

Fig. 5 (continued)

passed through the urban area of Ürümqi, which may result in the input of desert dust and some anthropogenic pollution. Thus, the concentrations of SO_4^{2-}, NO_3^-, and Ca^{2+} were very high. (2) Air masses arrived at July 26–28 and July 31, represented the long-range aerosol transport of air masses originated from Siberia and the Ural Mountain. The lower concentrations of NO_3^-, NH_4^+, and even the lowest total ions on July 31 may attribute to these cleaner air masses. (3) Air masses arrived at August 1–2, originated from the Caspian Sea, passed through the arid-regions of Uzbekistan and Kyrgyzstan and the northern region of Taklamakan Desert, arrived at the sampling site from southwest. These air masses resulted in the higher concentrations of cations.

Besides, the relative contributions of individual aerosol particles were also calculated then according to the three trajectory types classified above. Table 4 presents the numbers and relative abundance of aerosol particles at different air masses, which were simply represented by T1, T2, and T3. Variations of the individual aerosol particles were found to coincide with variability of the water-soluble ions encountered at different backward air mass trajectories. Total particle number distributions indicated that air masses in T2 were the cleanest air masses which resulted in the least particle numbers and almost lowest ion concentrations on July 26–28 and 31, while the highest particle numbers at T1 coincide with the highest ion concentrations on July 29–30 and August 3–4. The relative concentrations of mineral particles, soot, fly ashes, and other particles also revealed that back air mass trajectories crossed over Ürümqi on July 29–30 and August 3–4 resulted in the highest abundance of anthropogenic particles such as soot and fly ash particles. It validated the transport of anthropogenic pollutions from Ürümqi to this glacier site. However, the most abundant of mineral particles at these three different types of backward air mass trajectories suggested that the natural processes were still the primary sources of the aerosols over Mt. Bogda. It can be seen that although the air masses originated from different sources, they all passed through the arid and semi-arid regions of Central Asia, which may contribute to the abundant mineral particles. Previous research has also shown that synoptic processes favorable in the Tianshan occurred from

Table 4 Numbers and relative abundance of aerosol particles under different air masses arrived at the sampling site

Trajectory types[a]	Total numbers	Mineral particles		Soot		Fly ash		Other particles[b]	
		Number	Abundance (%)	Number	Abundance (%)	Number	Abundance (%)	Number	Abundance (%)
T1	868	624	71.9	177	20.4	51	5.9	16	1.8
T2	289	263	91.0	18	6.2	7	2.4	1	0.3
T3	343	297	86.6	31	9.0	12	3.5	3	0.9

[a]T1 represents the air masses that arrived on July 29–30 and August 3–4; T2 represents the air masses that arrived on July 26–28 and July 31; T3 represents the air masses that arrived on August 1–2

[b]Other particles are Fe-rich particles and little unrecognized particles

the west, suggesting that aerosol particles from western Kyrgyzstan, Kazakhstan, Uzbekistan, and Turkmenistan may be transported to the east (Aizen et al. 2004).

Conclusions

Intensive sampling experiment for aerosols conducted from July 26 to August 4 in 2009 provides the first information of the atmosphere over Mt. Bogda on the eastern Tianshan. Inorganic ion chemistry and individual particle characteristics of the aerosols were analyzed through ion chromatography and FESEM-EDX, respectively.

The results showed that SO_4^{2-} and NO_3^- were the dominant anions, and Ca^{2+} was the dominate cation in this region. The mean equivalent ratio of cations to anions was 1.05 close to 1.0, suggested that almost all of the ions had been quantified. The relationship between the eight inorganic ion species and their origins were also discussed. Natural mineral sources were the main contributor to most of the aerosol contents of Ca^{2+}, SO_4^{2-}, Na^+, Cl^-, and K^+ at this region, while NH_4^+ and NO_3^- were likely originated from anthropogenic activates. In comparison with the urban (Ürümqi) and remote (Akdala) sites of Xinjiang Uygur Autonomous Region, it was found that the major ion concentrations were much lower than those in Ürümqi, and some of the ions even lower than that in the background area of Akdala, indicating that the air quality of this galcierized region was still controlled by the natural processes.

Individual particle analysis provided detailed information on aerosol particles over Mt. Bogda. Based on the morphology and elemental compositions, particles were classed into four major groups: soot, fly ash, mineral particles, and little other matters (Fe-rich particles and unrecognized particles). Higher abundance of soot and fly ash particles emitted from anthropogenic activities, suggesting the impact of anthropogenic pollution during the study. However, almost 78.9% of the detected particles were mineral particles like alumosilicates, quartz, gypsum, calcite, etc., suggesting that natural dust processes were the primary sources of aerosols over this region, which coincided with the ionic analysis.

Backward air mass trajectory analysis indicated that air masses coming from the northwest and west account for the air quality during the sampling period. The arid and semi-arid regions of Central Asia were the major sources of mineral particles of this region. Transport pathways passed over the urban area of Ürümqi contributed to the little higher concentrations of NO_3^- and the higher occurrence of soot and fly ash particles emitted form the anthropogenic activities. This study has provided important insight into dust influence and anthropogenic pollutions in the eastern Tianshan in summer; however, other measurements are needed to determine their quantitative impacts on the enhanced melting and glacier retreating over this region.

Acknowledgements We would like to thank the two anonymous reviewers who have contributed valuable comments to improve the manuscript. This research was supported by the National Basic Research Program of China (no. 2010CB951003), Knowledge Innovation Programs of the Chinese Academy of Sciences (no. KZCX2-YW-127), and the National Natural Science Foundation of China (no. 40631001, 40571033, 40701034, 40371028, J0630966, 40701035). Support for this research has been provided under the Program for Glacier Processes Investigation (PGPI) conducted by the Tianshan Glaciological Station (TGS), Chinese Academy of Sciences (CAS). We also thank Professor Hu Kelin for the language editing and Zhu Yuman for the chemical analysis.

References

Aizen, V. B., Aizen, E. M., Melack, J. M., Kreutz, K. J., & Cecil, L. D. (2004). Association between atmospheric circulation patterns and firn-ice core records from the Inilchek glacierized area, Central Tien Shan, Asia. *Journal of Geophysical Research, 109*, D08304. doi:10.1029/2003JD003894.

Arimoto, R., Duce, R. A., Savoie, D. L., Prospero, J. M., Talbot, R., Cullen, J. D., et al. (1996). Relationships among aerosol constituents from Asia and the North Pacific during Pem-West A. *Journal of Geophysical Research, 101*(D1), 2011–2023.

Arimoto, R., Kim, Y. J., Kim, Y. P., Quinn, P. K., Bates, T. S., Anderson, T. L., et al. (2006). Characterization of Asian dust during ACE-Asia. *Global and Planetary Change, 52*, 23–56.

Bhaskar, B. V., Jeba Rajasekhar, R. V., Muthusubramanian, P., & Kesarkar, A. P. (2009). Ionic and heavy metal composition of respirable particulate in Madurai, India. *Environmental Monitoring and Assessment*. doi:10.1007/s10661-009-0895-8.

Buseck, P. R., & Pósfai, M. (1999). Airborne minerals and related aerosol particles: Effects on climate and the environment. *Proceedings of the National Academy of Sciences of the United States of America, 96*, 3372–3379.

Chakrabarty, R. K., Moosmuller, H., Garro, M. A., Arnott, W. P., Walker, J., Susott, R. A., et al. (2006). Emissions from the laboratory combustion of wildland fuels: Particle morphology and size. *Journal of Geophysical Research-Atmospheres, 111*(D7). doi:10.1029/2005JD006659.

Claquin, T., Schulz, M., & Balkanski, Y. J. (1999). Modeling the mineralogy of atmospheric dust sources. *Journal of Geophysical Research, 104*(D18), 22243–22256.

Cong, Z., Kang, S., & Qin, D. (2009). Seasonal features of aerosol particles recorded in snow from Mt. Qomolangma (Everest) and their environmental implications. *Journal of Environmental Sciences, 21*, 914–919.

Cong, Z., Kang, S., Dong, S., Liu, X., & Qin, D. (2010). Elemental and individual particle analysis of atmospheric aerosols from high Himalayas. *Environmental Monitoring and Assessment, 160*, 323–335.

Draxler, R. R., & Rolph, G. D. (2003). *HYSPLIT (Hybrid Single-Particle Lagrangian Integrated Trajectory) model access via NOAA ARL READY website*. NOAA Air Resources Laboratory, Silver Spring, MD. http://www.arl.noaa.gov/ready/hysplit4.html.

Gao, Y., Anderson, J., & Hua, X. (2007). Dust characteristics over the North Pacific observed through shipboard measurements during the ACE-Asia experiment. *Atmospheric Environment, 41*, 7907–7922.

Hoornaert, S., Godoi, R. H. M., & Grieken, R. V. (2004). Elemental and single particle aerosol characterisation at a background station in Kazakhstan. *Journal of Atmospheric Chemistry, 48*, 301–315.

Hou, S., Qin, D., Ren, J., Sheng, W., & Chen, T. (1999). The present environmental processes of ice core pH and conductivity records: A case study at the headwaters of Ürümqi river. *Journal of Glaciology and Geocryology, 21*, 371–379.

Hu, R. (2004). *Physical geography of the Tianshan mountains in China*. Beijing: China Environmental Science Press.

Hu, T., Lee, S., Cao, J., Chow, J. C., Watson, J. G., Ho, K., et al. (2009). Characterization of winter airborne particles at Emperor Qin's Terra-cotta Museum, China. *The Science of the Total Environment, 407*, 5319–5327.

Khoder, M. I., & Hassan, S. K. (2008). Weekday/weekend differences in ambient aerosol level and chemical characteristics of water-soluble components in the city centre. *Atmospheric Environment, 42*, 7483–7493.

Kreutz, K. J., & Sholkovitz, E. R. (2000). Major element, rare earth element, and sulfur isotopic composition of a high elevation firn core: Sources and transport of mineral dust in Central Asia. *Geochemistry Geophysics Geosystems, 1*, 2000GC000082.

Kreutz, K. J., Aizen, V. B., Cecil, L. D., & Wake, C. P. (2001). Oxygen isotopic and soluble ionic composition of a shallow firn core, Inilchek glacier, central Tien Shan. *Journal of Glaciology, 47*(159), 548–554.

Laluraj, C. M., Krishnan, K. P., Thamban, M., Mohan, R., Naik, S. S., D'Souza, W., et al. (2009). Origin and characterisation of microparticles in an ice core from the Central Dronning Maud Land, East Antarctica. *Environmental Monitoring and Assessment, 149*, 377–383.

Lee, X., Qin, D., Jiang, G., & Zhou, H. (2003). Atmospheric pollution of a remote area of Tianshan Mountain: Ice core record. *Journal of Geophysical Research, 108*(D14), 4406. doi:10.1029/2002JD002181.

Li, J., Zhang, G., Li, X., Yu, S., & Wu, Y. (2005). Analysis of seasonal variation of PM10 concentration and morphology: Taking Tianshan District, Ürümqi in 2004 as example. *Urban Environment & Urban Ecology, 18*(6), 16–18.

Li, J., Zhuang, G., Huang, K., Lin, Y., Xu, C., & Yu, S. (2008). Characteristics and sources of air-borne particulate in Ürümqi, China, the upstream area of Asia dust. *Atmospheric Environment, 42*, 776–787.

Li, Z., Li, K., & Wang, L. (2010). Study on recent glacier changes and their impact on water resources in Xinjiang, North Western China. *Quaternary Sciences, 30*(1), 96–106.

Liu, B. Y. H., Pui, D. Y. H., & Rubow, K. L. (1984). Characteristics of air sampling filter media. Aerosols in the mining and industrial work environments. In V. A. Marple, & B. Y. H. Liu (Eds.), *Instrumentation* (Vol. 3, pp. 989–1038). Newton, MA: Butterworth-Heinemann.

Mamane, Y., & Gottlieb, J. (1992). Nitrate formation on sea-salt and mineral particles-a single particle approach. *Atmospheric Environment, 26A*, 1763–1769.

Mamtimin, B., & Meixner, F. X. (2007). The characteristics of air pollution in the semi-arid city of Ürümqi (NW China) and its relation to climatological process. *Geophysical Research Abstracts, 9*, 06537.

Marenco, F., Bonasoni, P., Calzolari, F., Ceriani, M., Chiari, M., Cristofanelli, P., et al. (2006). Characterization of atmospheric aerosols at Monte Cimone, Italy, during summer 2004: Source apportionment and transport mechanisms. *Journal of Geophysical Research, 111*(D24202). doi:10.1029/2006JD007145.

Mayewski, P. A., Meeker, L. D., Whitlow, S., Twickler, M. S., Morrison, M. C., Alley, R. B., et al. (1993). The atmosphere during the younger dryas. *Science, 261*, 192–197.

Ming, J., Zhang, D., Kang, S., & Tian, W. (2007). Aerosol and fresh snow chemistry in the East Rongbuk Glacier on the northern slope of Mt. Qomolangma (Everest). *Journal of Geophysical Research, 112*, D15307. doi:10.1029/2007JD008618.

Ming, J., Xiao, C., Cachier, H., Qin, D., Qin, X., Li, Z., et al. (2009). Black Carbon (BC) in the snow of glaciers in west China and its potential effects on albedos. *Atmospheric Research, 92*, 114–123.

Okada, K., & Kai, K. J. (2004). Atmospheric mineral particles collected at Qira in the Taklamakan Desert, China. *Atmospheric Environment, 38*, 6927–6935.

Olivier, S., Schwikowski, M., Brütsch, S., Eyrikh, S., Gäggeler, H. W., Lüthi, M., et al. (2003). Glaciochemical investigation of an ice core from Belukha glacier, Siberian Altai. *Geophysical Research Letters, 30*(19), 2019. doi:10.1029/2003GL018290.

Paoletti, L., De Berardis, B., & Diociaiuti, M. (2002). Physico-chemical characterisation of the inhalable particulate matter (PM_{10}) in an urban area: An analysis of the seasonal trend. *Science of the Total Environment, 292*, 265–275.

Qu, W., Zhang, X., Arimoto, R., Wang, Y., Wang, D., Sheng, L., et al. (2009). Aerosol background at two remote CAWNET sites in western China. *Science of the Total Environment, 407*, 3518–3529.

Qu, W., Wang, D., Wang, Y., Sheng, L., & Fu, G. (2010). Seasonal variation, source, and regional representativeness of the background aerosol from two remote sites in western China. *Environmental Monitoring and Assessment, 167*, 265–288.

Reid, E. A., Reid, J. S., Meier, M. M., Dunlap, M. R., Cliff, S. S., Broumas, A., et al. (2003). Characterization of African dust transport to Puerto Rica by individual particle and size segregated bulk analysis. *Journal of Geophysical Research, 108*(D19), 8591.

Sharma, S., & Srinivas, M. (2009). Study of chemical composition and morphology of airborne particles in Chandigarh, India using EDXRF and SEM techniques. *Environmental Monitoring and Assessment, 150*, 417–425.

Shen, Z., Cao, J., Arimoto, R., Han, Z., Zhang, R., Han, Y., et al. (2009). Ionic composition of TSP and $PM_{2.5}$ during dust storms and air pollution episodes at Xi'an, China. *Atmospheric Environment, 43*, 2911–2918.

Shi, Z. B., Shao, L. Y., Jones, T. P., Whittaker, A. G., Lu, S. L., Bérubé, K. A., et al. (2003). Characterization of airborne individual particles collected in an urban area, a satellite city and a clean air area in Beijing, 2001. *Atmospheric Environment, 37*, 4097–4108.

Srivastava, A., Jain, V., & Srivastava, A. (2009). SEM-EDX analysis of various sizes aerosols in Delhi India. *Environmental Monitoring and Assessment, 150*, 405–416.

Sun, J., Qin, D., Mayewski, P. A., Dibb, J. E., Whitlow, S., Li, Z., et al. (1998). Soluble species in aerosol and snow and their relationship at Glacier 1, Tien Shan, China. *Journal of Geophysical Research, 103*(D21), 28021–28028.

Takeuchi, N., & Li, Z. (2008). Characteristics of surface dust on Ürümqi Glacier No. 1 in the Tien Shan Mountians, China. *Arctic, Antarctic, and Alpine Research, 40*(4), 744–750.

Verma, S. K., Deb, M. K., Suzuki, Y., & Tsai, Y. I. (2010). Ion chemistry and source identification of coarse and fine aerosols in an urban area of eastern central India. *Atmospheric Research, 95*, 65–76.

Wake, C. P., Mayewski, P. A., & Spencer, M. J. (1990). A review of Central Asian glaciochemical data. *Annals of Glaciology, 14*, 301–306.

Wake, C. P., Mayewski, P. A., Wang, P., Yang, Q., Han, J., & Xie, Z. (1992). Anthropogenic sulfate and Asian dust signals in snow from Tien Shan, northwest China. *Annals of Glaciology, 16*, 45–52.

Wang, Y., Zhuang, G., Tang, A., Yuan, H., Sun, Y., Chen, S., et al. (2005). The ion chemistry and the source of $PM_{2.5}$ aerosol in Beijing. *Atmospheric Environment, 39*, 3771–3784.

Wang, Y., Zhuang, G., Zhang, X., Huang, K., Xu, C., Tang, A., et al. (2006). The ion chemistry, seasonal cycle, and sources of $PM_{2.5}$ and TSP aerosol in Shanghai. *Atmospheric Environment, 40*, 2935–2952.

Williams, M. W., Tonnessen, K. A., Melack, J. M., & Yang, D. (1992). Sources and spatial variation of the chemical composition of snow in Tien Shan, China. *Annals of Glaciology, 16*, 25–37.

Wolff, E. W. (1996). The record of aerosol deposited species in ice core, and problem of interpretation. In E. W. Wolff, & R. Bales (Eds.), *Chemical exchange between the atmosphere and polar snow* (pp. 1–17). New York: Springer.

Wu, G., Ageta, Y., & Qiu, J. (1983). Physical geographic features and climatic conditions of glacial development in Bogda Area, Tian Shan. *Journal of Glaciology and Geocryology, l5*(3), 5–16.

Wu, D., Tie, X., & Deng, X. (2006). Chemical characterizations of soluble aerosols in southern China. *Chemosphere, 64*, 749–757.

Xie, R. K., Seip, H. M., Leinum, J. R., Winje, T., & Xiao, J. S. (2005). Chemical characterization of individual particles (PM_{10}) from ambient air in Guiyang City, China. *Science of the Total Environment, 343*, 261–272.

Xie, R. K., Seip, H. M., Liu, L., & Zhang, D. S. (2009). Characterization of individual airborne particles in Taiyuan City, China. *Air Quality, Atmosphere and Health, 2*, 123–131.

Xu, B., Cao, J., Hansen, J., Yao, T., Joswia, D. R., Wang, N., et al. (2009). Black soot and the survival of Tibetan glaciers. *Proceedings of the National Academy of Sciences of the United States of America, 106*(52), 22114–22118.

Yue, W., Li, X., Liu, J., & Li, Y. (2006). Characterization of $PM_{2.5}$ in the ambient air of shanghai city by analyzing individual particle. *Science of the Total Environment, 368*, 916–925.

Zhang, K., Li, Z., Wang, F., & Li, C. (2008). Soluble mineral dusts in aerosol and surface snow on the Glacier No. 1 at the headwaters of Ürümqi River, east Tianshan Mountains: Characteristics and their interrelation-taking calcium and magnesium as examples. *Journal of Glaciology and Geocryology, 31*(1), 113–118.

Zhao, Z., & Li, Z. (2004). Determination of soluble ions in atmospheric aerosol by ion chromatography. *Modern Scientific Instruments, 5*, 46–49.

Zhao, Z., Li, Z., Edwards, R., & Wang, F. (2006). Atmosphere-to-snow-to-firn transfer of NO_3^- on Glacier No. 1, eastern Tien Shan, China. *Annals of Glaciology, 43*, 239–244.

Zhao, Z., Tian, L., Fischer, E., Li, Z., & Jiao, K. (2008). Study of chemical composition of precipitation at an alpine site and a rural site in the Ürümqi River valley, Eastern Tien Shan, China. *Atmospheric Environment, 42*(39), 8934–8942.